Dairy Sci. Technol. 88 (2008) 31–43

DOI: 10.1051/dst:2007006

Available online at:
www.dairy-journal.org

Original article

Residence time distribution: a tool to improve spray-drying control

Romain JEANTET[1]*, Fabrice DUCEPT[1,2], Anne DOLIVET[1], Serge MÉJEAN[1,3], Pierre SCHUCK[1]

[1] Agrocampus Rennes, INRA, UMR1253, Science et Technologie du Lait et de l'Œuf, 35000 Rennes, France
[2] AgroParisTech, CEMAGREF, INRA, UMR1145 Génie Industriel Alimentaire, 1 avenue des Olympiades, 91744 Massy Cedex, France
[3] BIONOV, 85 rue de Saint-Brieuc, 35042 Rennes cedex, France

Abstract – Dairy powders are mainly obtained by spray drying, which is an effective process as it makes possible long-term storage at an ambient temperature. However, the control and design of this operation is still based on empirical knowledge. Improvement in product quality, which is governed by time/temperature history, thus involves greater understanding of the process via physico-chemical, thermodynamic and kinetic approaches. With regard to the latter, the residence time distribution (RTD) of the product provides valuable information about the product flow pattern in the dryer according to the operating conditions. The aim of this study was to determine the RTD of skim milk in a drying plant with different configurations, according to fine particle recycling (top of the chamber or internal fluid bed) and internal fluid bed thickness (4 to 16 cm). The RTD signal of the atomisation device was established first; then the RTD signals of the different spray-dryer configurations were obtained by deconvolution of the experimental curves obtained and the RTD signal of the atomisation device, and modelled according to a combination of four reactor sets. The mean residence time of the product was only slightly modified by the dryer configuration (range 9.5 to 12 min). However, the results showed that a thicker internal fluid bed tends to increase mean residence time due to higher product retention, whereas top recycling of fine particles tends to decrease the mean residence time because of better agglomeration. RTD modelling provides additional information concerning the product flow rate fraction and the residence time distribution of each part of the dryer (chamber, cyclones and fluid bed), indicating that 60 to 80% of the powder passes through the cyclones, depending on the configuration. This study provides greater understanding of dryer operation, and allows further correlation between process parameters and biochemical changes (protein denaturation, Maillard reaction, etc.).

residence time distribution / spray drying / dairy powders

摘要 – 喷雾干燥器的停留时间分布对干燥产品质量的影响。喷雾干燥能有效延长产品在常温下的保藏期, 常应用于乳粉的干燥中。但是, 目前喷雾干燥的操作和设计完全根据经验; 提高产品质量全依靠改变时间/温度的设置, 对喷雾干燥过程的研究则常常运用物理化学、热力学和动力学方法。至于后者, 可以利用产品停留时间分布在干燥器里运行的流动模型所提供的有用信息。本文旨在通过调整物料的微粒循环 (塔顶或内流化床) 和内流化床的物料厚度 (4–16 cm), 测定不同构型的干燥设备中脱脂乳的停留时间分布。首先确定雾化设备的停留时间分布信号, 然后运用反褶积方法对停留时间分布曲线进行分析, 得到不同构型干燥塔和雾化器的停留时间分布信号, 将这四组停留时间分布数据进行组合建立模型, 发现改变干燥塔的构型,

* Corresponding author (通讯作者): romain.jeantet@agrocampus-rennes.fr

平均停留时间仅发生了微小的变化 (在 9.5–12 min); 但是, 物料堆积越厚的内流化床对产品的吸附力越大, 停留时间越长; 而顶端物料微粒循环由于凝结作用, 使得平均停留时间缩短。由停留时间分布模型还可以看出产品流动速率分数和干燥设备各部件 (干燥塔、旋风分离器、流化床) 的停留时间分布情况, 依构型的不同, 一般有 60%–80% 的脱脂乳粉经过旋风分离器。本研究加深了对喷雾干燥器操作的理解, 有利于对工艺参数与产品生化变化 (蛋白变性、美拉德反应等) 的关系进一步深入研究。

停留时间分布 / 喷雾干燥 / 乳粉

Résumé – Distribution des temps de séjour en séchage par pulvérisation de lait écrémé. La technique la plus employée pour la déshydratation des produits laitiers est le séchage par atomisation, qui permet le report des produits sur de longues durées à température ambiante. Cependant, le contrôle de cette opération est encore fondé sur des savoir-faire empiriques, et l'amélioration de la qualité des poudres, qui dépend notamment des couples temps/température subis, nécessite aujourd'hui une démarche plus rigoureuse basée sur des approches physico-chimiques, thermodynamiques et cinétiques. À ce titre, la détermination de la distribution des temps de séjour (DTS) permet d'obtenir une modélisation des flux produits au sein du séchoir, en fonction des conditions opératoires. L'objectif de cette étude était de déterminer la DTS du lait écrémé au sein d'une tour de séchage pilote sous différentes configurations, en fonction de la zone de recyclage des fines (haut de tour ou lit fluidisé interne) et de l'épaisseur du lit fluidisé interne (4 à 16 cm). Les fonctions DTS correspondant aux différentes configurations ont été déterminées par déconvolution des courbes expérimentales obtenues et de la fonction DTS du système d'atomisation, établie dans un premier temps ; ces fonctions ont ensuite été modélisées à partir d'une combinaison de quatre ensembles de réacteurs agités. Le temps de séjour moyen du produit est faiblement modifié par la configuration mise en œuvre, et varie de 9,5 à 12 min. Cependant, nos résultats montrent qu'un lit fluidisé interne plus épais tend à accroître le temps de séjour moyen du fait d'une rétention accrue du produit, tandis que le recyclage des fines en haut de tour le diminue. La modélisation des signaux DTS apporte des informations supplémentaires concernant la fraction de débit massique et le temps de séjour du produit circulant dans les différentes parties du séchoir (chambre, cyclones, lit fluidisé) : selon la configuration, 60 à 80 % de la poudre transiterait au travers des cyclones. Ces résultats contribuent à une meilleure compréhension du fonctionnement du séchoir, et permettent d'envisager des corrélations ultérieures entre paramètres du procédé et modifications biochimiques (dénaturation des protéines, réaction de Maillard, etc.).

distribution des temps de séjour / séchage par atomisation / poudres laitières

1. INTRODUCTION

Most dairy powders are currently obtained by spray drying, which consists of spraying the concentrated dairy liquid (skim and whole milk, whey, dairy fractions resulting from membrane filtration and chromatographic separation) in droplets of about 50 μm diameter into a large drying chamber where it is mixed with air heated to 200 °C. As the droplet dries, its temperature gradually rises from the wet bulb temperature until it reaches the temperature of the surrounding outlet air, i.e. it remains below 100 °C. Classical spray-dryers are combined with a fluid bed, which usually agglomerates the fine powder coming from the drying chamber in the wet zone, completes the drying process and cools the powder. In recent 3-stage installations, another fluid bed (internal) with agglomeration and additional drying functions is included at the bottom of the drying chamber [4, 9].

The final powder quality includes general properties (moisture content and biochemical composition, water activity, sensorial quality, etc.) and properties depending on the process parameters (rehydration, constituent denaturation, granulometry, flowability, floodability, hygroscopicity, stickiness, cakiness,

density and colour). These latter properties are mainly determined first by the agglomeration process and then by the time/temperature history of the product in the system, including the preliminary steps (heat treatment, membrane separation, evaporation, etc.). They are also dependent on the water content, because droplet temperature and water content are connected. Moreover, the rate of enzymatic and chemical changes depends on factors such as water content, temperature and time. It is therefore necessary to consider these three parameters in order to control thermal damage of constituents and process-dependent properties. Since drying occurs within a few seconds, the thermal damage is often considered as limited. However, the flow pattern of 2- and 3-stage installations (including recycling of fine particles) results in a longer processing time, and makes it difficult to predict the residence time distribution of the product in the dryer, because of varying particle sizes and unknown recirculation.

Moreover, the control and design of this operation is still based on empirical knowledge and relies heavily on user and designer experience [5]. There have been few scientific studies to date making it possible to optimise drying operating conditions and equipment design in terms of energy costs and powder quality [6]. Some recent publications have proposed tools based on physico-chemical and thermodynamic findings in order to prevent sticking in the drying chamber and to control powder quality [7]. Different methods can be considered in order to determine the residence time of the product in the system, which is a necessary step for drying control. Computational fluid dynamics (CFD) allow study of the consequences of modifications in operating conditions (temperature, flow rate) and process configuration with regard to particle characteristics (temperature, water content) and trajectories in the dryer [3, 10]. On the basis of process knowledge, and by using appropriate physical laws, this numerical approach can provide very precise local information. However, the model construction needs subsequent simplifications involving either the evolution of the product characteristics (e.g., density or porosity) or the process (heat or mass transfer laws). Moreover, several experiments are required to determine unknown model parameters and to verify hypotheses (boundary conditions), and model validation therefore remains difficult.

However, determination of the product residence time distribution (RTD) is an overall and experimental approach which provides valuable information about the product flow pattern in the dryer, according to the operating conditions [11, 12]. It consists of following a tracer introduced before the dryer inlet until the dryer outlet; the signal obtained can be numerically deconvoluted in order to provide specific RTD signals of the different sections of the equipment. It does not provide a physical understanding of the operation as CFD does, but on the other hand, it integrates the product and process complexity fully. In this sense, this method provides overall understanding and management of the flow pattern in the dryer, as well as additional information on CFD in order to optimise drying operating conditions and equipment design. Moreover, measurement of RTD in a dryer plant has never been previously published to our knowledge.

The aim of this study was to determine the RTD of the skim milk in a drying plant with different drying configurations, with regard to the recycling of fine particles (top of the chamber or internal fluid bed) and the internal fluid bed thickness. The RTD signals obtained corresponded to the overall response of the dryer. Their modelling was then undertaken according to a combination of plug flow reactors in order to obtain a physical interpretation of the

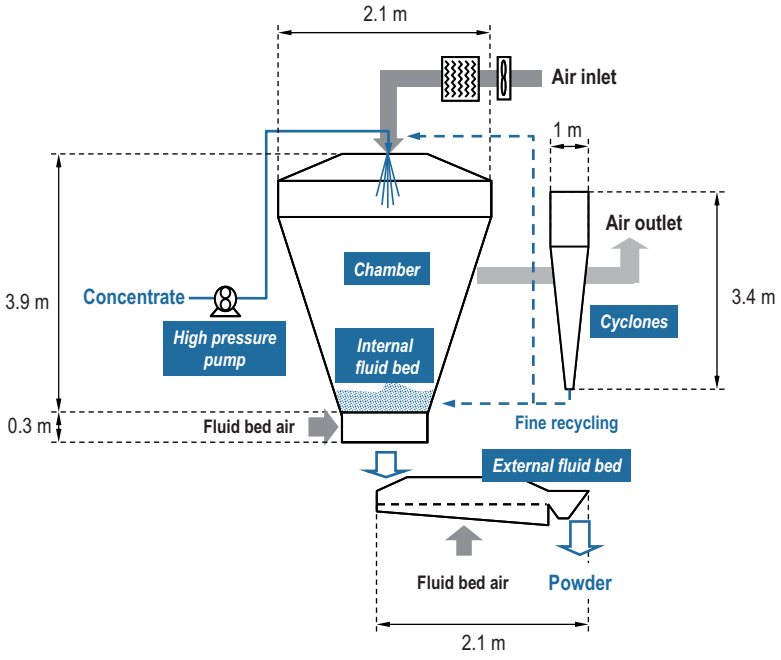

Figure 1. 3-Stage spray dryer pilot.

operation of each dryer section (chamber, internal fluid bed, cyclones, etc.).

2. MATERIALS AND METHODS

2.1. Spray-drying experiments

Skim milk powder was recombined into 40 (±1)% (w/w) dry matter prior to drying. Spray drying was performed at Bionov (Rennes, France) in a 3-stage spray-dryer plant with an evaporation capacity of 70 to 100 kg·h^{-1} (Fig. 1; GEA, Niro Atomiser, St Quentin-en-Yvelines, France), according to Schuck et al. [8]. Five experiments were performed, corresponding to different spray-drying configurations related to fine particle recycling (top of the chamber or internal fluid bed) and the internal fluid bed thickness (thin or thick; Tab. I and Fig. 2). Configuration ❸ was tested twice, in order to assess the experimental reproducibility. The atomiser was equipped with a pressure nozzle (0.73 mm diameter orifice; n°69) and a 4-slot core (0.51 mm nominal width; n°421), providing a 60° spray angle. The temperature of the concentrate before drying was 50 °C, and the concentrate flow rate was 94.5 ± 5.6 L·h^{-1}. The inlet air flow rate and outlet air temperature were 3715 ± 101 kg·h^{-1} and 88.0 ± 0.7 °C, respectively. The internal fluid bed temperature and external fluid bed temperature (first and second part) were 74.3 ± 0.3 °C, 34.4 ± 0.3 °C and 19.9 ± 0.1 °C, respectively.

2.2. Chemical and physical analysis

Solid concentration and free moisture content were calculated according to weight loss after drying 1.5 g of the

Table I. Experimental spray drying conditions.

Configuration	Fine particle recycling position	Fluid bed	Fluid bed thickness (cm)	Inlet air temperature (°C)	Inlet air AH (g water·kg^{-1} dry air)	Outlet air AH (g water·kg^{-1} dry air)	Atomization pressure (MPa)	Powder temperature on fluid bed (°C)
❶	Internal fluid bed	Thin	4 (± 1)	185.2 (± 0.1)	4.5 (± 0.1)	21.2 (± 0.7)	10.5 (± 0.5)	68.4 (± 1.1)
❷	Top of the chamber	Thick	16 (± 3)	191.6 (± 0.6)	5.1 (± 0.1)	21.2 (± 0.6)	10.5 (± 0.5)	77.0 (± 2.0)
❸	Top of the chamber	Thin	4 (± 1)	191.6 (± 0.6)	5.2 (± 0.1)	21.5 (± 0.6)	10.5 (± 0.5)	73.4 (± 2.0)
			4 (± 1)	191.6 (± 1.7)	8.2 (± 0.2)	24.7 (± 0.7)	10.5 (± 0.5)	77.7 (± 0.6)
❹	Internal fluid bed	Thick	14 (± 2)	187.1 (± 1.0)	7.2 (± 0.2)	26.3 (± 0.6)	11.8 (± 0.4)	69.8 (± 0.3)

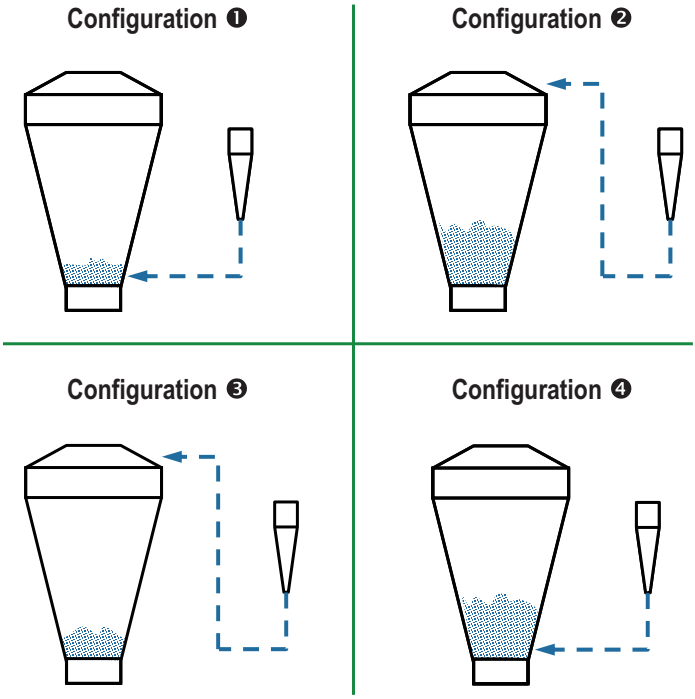

Figure 2. Spray drying configurations according to fine particle recycling (top of chamber or internal fluid bed) and internal fluid bed thickness (thin or thick).

sample mixed with sand in a forced air oven at 105 °C for 5 h (powder) or 7 h (concentrate). Sodium chloride content (NaCl) was based on chloride measurement, and determined by conductimetry using a silver electrode (Corning 926, Humeau, La Chapelle, France). Powder particle $D_{(0.5)}$ diameter (median diameter) measurements were assessed by laser granulometry (Mastersizer 2000, Malvern Instruments, Malvern, UK) and the uniformity index was calculated according to Carr [2].

2.3. Determination of RTD and modelling

RTD characterisation was based on measurement of NaCl concentration; 20 kg of tracer, corresponding to a skim milk concentrate of 40% (w/w) dry matter to which 1.2% of NaCl were added, were used for each experiment. All the powder was collected at the dryer outlet for 80 min after tracer injection, each sample corresponding to the quantity of powder exiting every 2 min. Sodium chloride concentration at the inlet and the outlet was obtained by chloride measurement, and determined by conductimetry using a silver electrode. It was then possible to plot sodium chloride concentrations according to time. The tracer was placed in a tank connected to the feed line with a three-way valve, so that the shape of the injection signal could be considered as square.

In order to determine the specific RTD function of the tower, we used the following experimental strategy. First, the RTD signal ($E_{ad}(t)$) of the atomisation

device (corresponding to injection pump, filters and nozzle) was established. After 2 min of tracer injection, the NaCl content was measured over time by the continuous and full sampling of skim milk at the nozzle outlet, on a 30-s period basis: this provided the experimental output signal ($y(t)$). $E_{ad}(t)$ was obtained by numerical deconvolution of $y(t)$ by the injection square signal ($x(t)$).

It was then possible to calculate the response of the atomisation device to a tracer injection of any sort. For a given tracer square signal ($\delta(t)$), the corresponding injection $x(t)$ signal at the atomisation device outlet (i.e., at the tower entrance) was obtained by convolution of $E_{ad}(t)$ and $\delta(t)$.

Finally, the $E(t)$ RTD signals of the spray-dryer in the different configurations were determined by numerical deconvolution of the experimental $y(t)$ output signal (corresponding to an experimental particle RTD of the complete system [atomisation device + tower]) and the $x(t)$ injection signal. Having determined $E(t)$, it was then possible to calculate the residence time of each fluid element, and conversely, the time, t, at which a certain fraction of the material entering at $t = 0$ is no longer present in the equipment. The mean residence time, τ, corresponds to the time when 50% of the material entering at $t = 0$ has passed through the equipment.

The modelling of the RTD functions by a combination of plug flow reactor sets was constructed on physical bases in order to take into account the fine particle recycling at the top of the chamber or internal fluid bed (model A or B; Fig. 3). Model A was used for fluid bed recycling: the product passes through the first reactor set, and then continues on its way with parallel recirculation in three other reactor sets. On the other hand, top recycling of fine particles corresponds to model B: the product passes through the first reactor set combined with parallel recirculation in the second reactor set, and then continues on its way with parallel recirculation in two other reactor sets.

Whatever the model, Q is the product flow rate through the equipment, and a_i refers to the Q fraction going into the i^{th} reactor set. Each reactor set includes J_i plug flow reactors in series, and can be characterised by a mean residence time (τ_i). Its own $E_i(t)$ RTD function is defined by:

$$E_i(t) = \left(\frac{J_i}{\tau_i}\right)^{J_i} \frac{t_i^{J_i-1} \exp(J_i t_i/\tau_i)}{(J_i - 1)!}. \qquad (1)$$

The number of plug flow reactor sets and the three parameters of each reactor set (a_i, J_i and τ_i) were adjusted step by step in order to correspond to the experimental $E(t)$ RTD functions obtained for the different configurations, according to model A (Eq. (2)) or B (Eq. (3)):

$$\begin{cases} E(t) = (1-a_4) \cdot E_b(t) + a_4 \cdot E_b(t) \otimes E_4(t) \\ E_b(t) = (1-a_3) \cdot E_a(t) + a_3 \cdot E_a(t) \otimes E_3(t) \\ E_a(t) = (1-a_2) \cdot E_1(t) + a_2 \cdot E_1(t) \otimes E_2(t) \end{cases} \qquad (2)$$

$$\begin{cases} E(t) = (1-a_4) \cdot E_b(t) + a_4 \cdot E_b(t) \otimes E_4(t) \\ E_b(t) = (1-a_3) \cdot E_a(t) + a_3 \cdot E_a(t) \otimes E_3(t) \\ E_a(t) = E_1(t) + (a_2 \cdot E_1(t) \otimes E_2(t)) \otimes E_1(t) \end{cases} \qquad (3)$$

where $\otimes$ is the convolution product.

It should be noted that 4 plug flow reactor sets are required and are sufficient for the modelling of $E(t)$, whatever the configuration. Model accuracy was evaluated by the standard deviation between the model and experimental RTD curves.

3. RESULTS AND DISCUSSION

3.1. Powders

The different powders obtained showed the same biochemical results, with no significant differences between powder a_w and dry matter (96.3 ± 0.8 %). $D_{(0.5)}$ diameter values were greater with top fine particle recirculation (configurations ❷ and ❸:

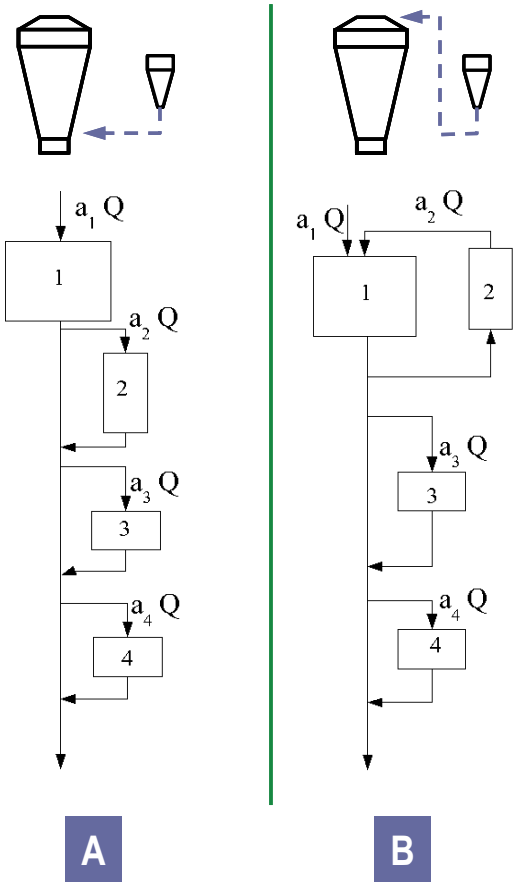

Figure 3. Plug flow reactor scheme used for RTD modelling. A: model corresponding to fluid bed recycling of fine particles; B: model corresponding to top recycling of fine particles.

$D_{(0.5)}$ = 196 ± 3 µm; uniformity index = 1.9) than with fluid bed recirculation (configuration ❶: $D_{(0.5)}$ = 158 µm; uniformity index = 2.3 / configuration ❹: $D_{(0.5)}$ = 109 µm; uniformity index = 2.0). This point is important because the smaller the powder diameter, the higher the powder flowability in the retention zones such as rotary discharge valves; it can thus affect the powder residence time distribution in the equipment. The difference observed can be explained by the fact that top fine particle recirculation increases agglomeration, a cloud of fine particles being formed in the direct environment of the liquid droplets. On the other hand, agglomeration is limited with fluid bed recirculation, in which case the fine particles are mixed with almost dried particles. The smaller $D_{(0.5)}$ value obtained for configuration ❹ can be attributed to the higher atomisation pressure in this case (Tab. I), resulting in smaller droplets during atomisation.

3.2. Atomisation device RTD

First, the RTD of the atomisation device was assessed. Figure 4a represents the 2-min tracer injection ($x(t)$) and the output

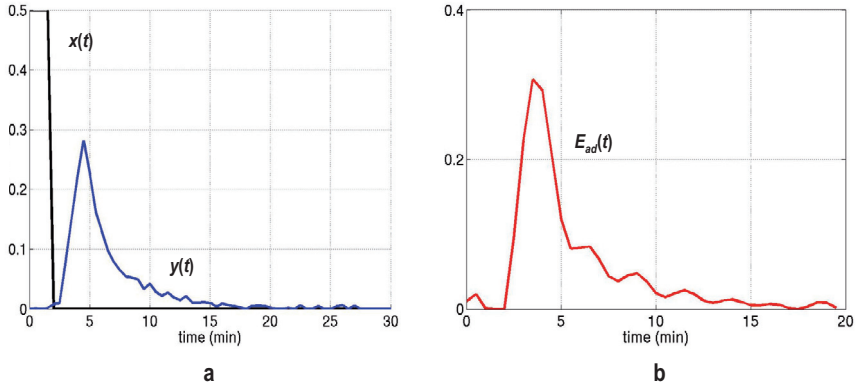

Figure 4. RTD determination of atomisation device. a: Tracer injection $x(t)$ and output signal $y(t)$; b: $E_{ad}(t)$.

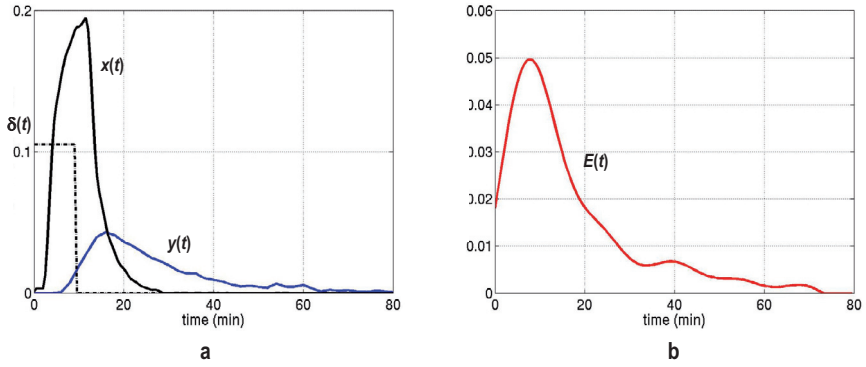

Figure 5. Determination of tower RTD for configuration ❶. a: Tracer square signal $\delta(t)$, injection signal $x(t)$ and output signal $y(t)$; b: $E(t)$.

signal ($y(t)$). The areas of $y(t)$ and $x(t)$ are normalised by the overall tracer mass. The deconvolution of $y(t)$ by $x(t)$ gives $E_{ad}(t)$ (Fig. 4b). As previously stated, this curve is a probability distribution: for example, the probability of a fluid element remaining in the atomisation device for 3 min is 0.2. The RTD signal increases rapidly at t_0 + 2.5 min, the maximum is reached at t_0 + 4 min and the trail ends at around 18 min. The mean residence time is 4.5 min.

3.3. Tower RTD

It is thus possible to simulate the $x(t)$ injection signal at the injection device outlet, i.e. the tower entrance. For configuration ❶ (thin fluid bed/fine particle recirculation on fluid bed), $x(t)$ was calculated by convolution of $E_{ad}(t)$ and the tracer $\delta(t)$ 10 min square signal: Figure 5a represents $\delta(t)$, $x(t)$ and the $y(t)$ output signal obtained for this configuration. Deconvoluting $y(t)$ by $x(t)$ gives the

RTD function $E(t)$ (Fig. 5b) for the tower. This figure shows that some powder particles leave the tower almost immediately, whilst others remain in the installation for more than 70 min (end of the trail). The mean residence time is 12 min for this configuration. This is in close agreement with the mean time of the output signal $y(t)$, which is here 22 min, and corresponds to the sum of the mean residence time of the square signal (5 min), the atomisation device RTD (4.5 min) and the tower RTD (12 min).

The $E(t)$ functions corresponding to configurations ❷ (Fig. 6a), ❸ (Fig. 6b) and ❹ (Fig. 6c) were obtained in the same way. Figure 6b shows $E(t)$ functions obtained for configuration ❸ in replicate, compared with that obtained for configuration ❶ (black dotted line). The reproducibility of the results is satisfactory, as the two curves are almost merged. From $E(t)$ functions, it is possible to determine the mean residence time (τ) for each configuration. τ is 12 min for configurations ❶ and ❷, 9.5–10 min for configuration ❸ and 11 min for configuration ❹.

It clearly shows that the mean residence time is in the same range whatever the configuration, as these differences are very small when compared with the time range of $E(t)$ functions (up to 70 min). However, the τ values can be discussed in relation to internal fluid bed thickness and to location of fine particle recycling.

Configurations ❷ and ❸ differ by internal fluid bed thickness. It can therefore be concluded that increasing the fluid bed thickness tends to increase the residence time. This can be explained by the fact that the internal fluid bed is a place where the powder remains for a certain time, and the thicker the fluid bed, the greater the mass of powder retained.

On the other hand, configurations ❶ and ❸ differed in the place where the fine particles were recycled. As compared with fine particle recycling on the fluid bed, the top recycling of fine particles greatly reduced the mean residence time. This can be attributed to better agglomeration, which reduces the trail of the RTD signal (Fig. 6b). These results were not expected, in the sense that adding a recirculation to the system configuration should result in longer residence time. This was probably due to the specific nozzle configuration of the dryer, where the fine particles are directly recycled on the spraying cone. In the case of an industrial drying plant, where the cloud of fine particles is recirculated in the environment of several nozzles, the fine particle agglomeration, and hence the benefit of top recycling on mean residence time, should be lower.

Finally, the medium τ value of configuration ❹, despite the thick fluid bed and fine particle recycling on the fluid bed, which corresponded to the most unfavourable configuration, could be attributed to the low $D_{(0.5)}$ value of the powder obtained in this case. Indeed, the fluid bed thickness was very difficult to maintain in this trial, because of lower retention of the powder by the rotary discharge valve at the fluid bed outlet. This result highlights the strong link between process parameters and product quality, a slight modification of one parameter (e.g., higher atomisation pressure) leading to a different product (reduced median diameter), and hence modified behaviour in the equipment (medium τ value).

3.4. RTD modelling

Table II gives the standard deviation between model and experimental RTD measurements for the different configurations considered. Table III gives the J_i, a_i and τ_i reactor set values obtained for the modelling of each configuration. The parameter values given for configuration ❸ (tested twice) correspond to the mean parameter value (± standard deviation). The accuracy

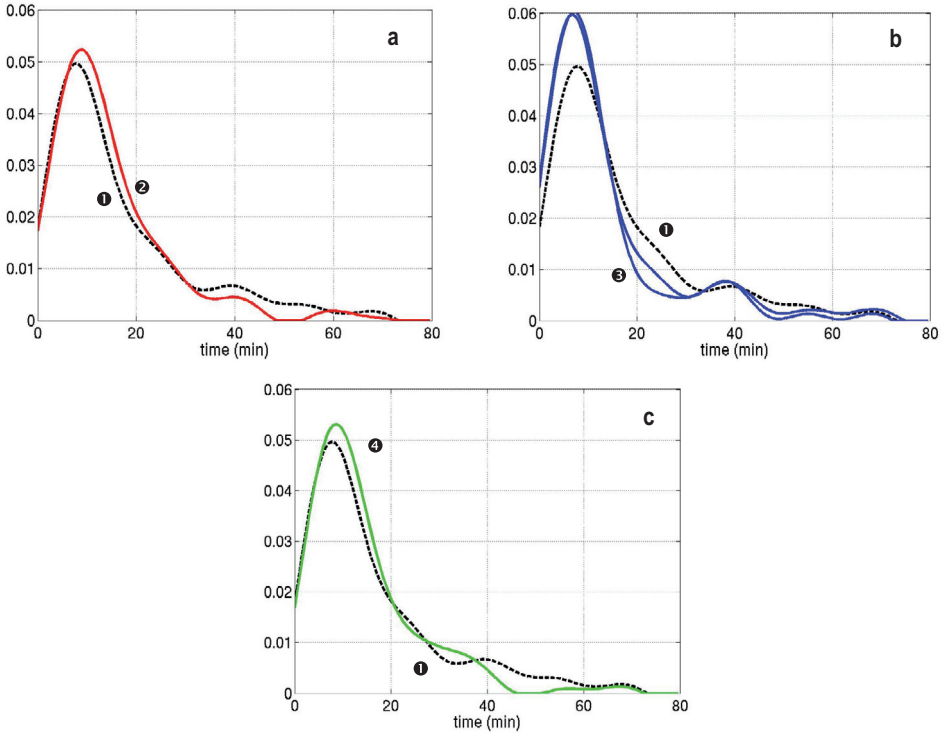

Figure 6. $E(t)$ function obtained for configurations ❷, ❸ and ❹, compared to configuration ❶ (dotted line). a: Configurations ❶ and ❷; b: configuration ❸ in replicate and configuration ❶; c: configurations ❶ and ❹.

Table II. Standard deviation of the model compared with the experimental curves.

Configuration	Standard deviation ($E(t)$ unit)
❶	0.002
❷	0.002
❸	0.003
❹	0.001

and reproducibility of the model is satisfactory, considering the very low standard deviations obtained.

In general, and considering one reactor set, the model parameter values were similar whatever the configuration. Nevertheless, certain differences can be discussed, in order to provide a physical understanding of the operation of each dryer section.

The a_i value of the first reactor set is one, which means that the whole product enters this reactor. It can therefore represent the chamber.

The τ_i values of the second reactor set range from 6 to 7 min for configurations ❶ and ❹ to 1 min for configurations ❷ and ❸. In other words, the ratio of first to second reactor set τ_i values is 6 for configurations ❷ and ❸. This is in close agreement with the measured fine particle recirculation flow rate (253 ± 12 kg·h^{-1}) to powder flow rate (close to 37 kg·h^{-1}) ratio, which is 6.7. The second reactor set could thus act as the cyclones and the fine

Table III. Model parameters.

		Reactor set			
Parameter	Configuration	1	2	3	4
J_i	❶	1	2	50	140
	❷	2	2	10	140
	❸	2 (± 0)	2 (± 0)	70 (± 0)	140 (± 0)
	❹	1	2	40	140
a_i	❶	1	0.8	0.10	0.09
	❷	1	0.6	0.15	0.05
	❸	1 (± 0)	0.6 (± 0.0)	0.08 (± 0.03)	0.11 (± 0.00)
	❹	1	0.8	0.11	0.09
τ_I (min)	❶	6	6	18	33
	❷	6	1	15	30
	❸	6 (± 0)	1 (± 0)	16 (± 2)	31 (± 0)
	❹	6	7	15	33

particle recirculation pattern. Regarding the a_i value of this reactor set, it can be assumed that 60% (configurations ❷ and ❸) to 80% (configurations ❶ and ❹) of the product would pass through the cyclones. The higher a_i value obtained for configurations ❶ and ❹ is in agreement with the lower agglomeration, i.e. the higher fine particle content, observed in this case. Finally, the high a_i values of the first and second reactor sets clearly indicate that the tower and the cyclones account for the greater part of the overall residence time distribution of the product.

The third reactor set shows lower J_i and higher a_i values for configurations ❷ and ❹ than for configurations ❶ and ❸. In addition, configuration ❷ shows lower J_i and higher a_i values than those of configuration ❹ (10 versus 40 and 0.15 versus 0.11, respectively). RTD theory indicates that increasing the J_i number of plug flow reactors in series tightens the residence time distribution and leads to piston flow, and conversely, that a lower J_i value expands the residence time distribution [1]. This is logical because with increasing values of J_i, the probability that a particle remains for a relatively short or relatively long period in all reactors becomes smaller. This reactor set could therefore correspond to the internal fluid bed, the increase in fluid bed thickness in configuration ❷ leading to the retention of a larger amount of product (higher a_i value) and thus to a wide residence time distribution (lower J_i value). Conversely, the J_i and a_i values of configuration ❹ correspond to lower powder retention in the fluid bed compared with configuration ❷, in agreement with our previous assumptions concerning the influence of granulometry on powder retention. However, it would be better to consider that the third reactor set is not limited to the single internal fluid bed but is fairly strongly influenced by it, as the model does not take into account the backflow of powder from the internal fluid bed towards the chamber.

Finally, the fourth reactor set, with an almost infinite number of reactors, may

correspond to the overall recirculation and flow in the equipment, which is piston type (high J_i value) with a mean residence time of 30 to 33 min.

4. CONCLUSIONS

To conclude, the RTD approach provides greater understanding of the drying operation, according to the process configurations considered in this paper.

Our results show that the mean residence time (τ) is only slightly modified by the changes in the dryer configuration considered here. Nevertheless, a thicker internal fluid bed results in a higher τ value because of higher product retention, whereas top recycling of fine particles decreases the τ value. We attribute this to better agglomeration, which reduces the stay of the fine particles in the dryer. RTD modelling provides additional information through J_i, a_i and τ coefficients, thus also providing a physical understanding of certain section operations according to dryer configuration. As RTD is a statistical representation of the residence time of the product in the equipment, it statistically describes the time/temperature the product is subjected to during treatment. This approach thus complements CFD, and can be useful for CFD validation.

The future prospects are at the level of combining this approach with the product temperature and water content in the dryer. These parameters can be accessed either by modelling or measurement, and will make it possible to describe the time/temperature history of the product, including the effects of pre-drying treatments by RTD measurement in concentration by evaporation, and to establish further correlations with changes in constituents and dependent powder properties.

REFERENCES

[1] Broyart B., Lameloise M.L., Dispersion des temps de séjour, in: Bimbenet J.J., Duquenoy A., Trystram G., Génie des procédés alimentaires - des bases aux applications, Dunod, Paris, 2002, pp. 288–304.

[2] Carr R.L., Evaluating flow properties of solids, Chem. Eng. 72 (1965) 163–168.

[3] Ducept F., Sionneau M., Vasseur J., Superheated steam dryer: simulations and experiments on product drying, Chem. Eng. J. 86 (2002) 75–83.

[4] Masters K., Spray Drying, Ed. Longman Scientific & Technical and John Wiley & Sons Inc., Essex, UK, 1991.

[5] Masters K., Scale-up of spray dryers, Drying Technol. 12 (1994) 235–257.

[6] Schuck P., Spray drying of dairy products: state of the art, Lait 82 (2002) 375–382.

[7] Schuck P., Méjean S., Dolivet A., Jeantet R., Thermo hygrometric sensor: a tool for optimizing the spray drying process, Innov. Food Sci. Emerging Technol. 6 (2005) 45–50.

[8] Schuck P., Roignant M., Brulé G., Méjean S., Bimbenet J.J., Caractérisation énergétique d'une tour de séchage par atomisation multiple effet, Ind. Alim. Agric. 115 (1998) 9–14.

[9] Sougnez M., L'évolution du séchage par atomisation, Chimie Magazine 1 (1983) 1–4.

[10] Verdurmen R.E.M., Straatsma H., Verschueren M., van Haren J.J., Smit E., Bergeman G., De Jong P., Modelling spray drying processes for dairy products, Lait 82 (2002) 453–463.

[11] Villermaux J., Génie de la réaction chimique - conception et fonctionnement des réacteurs, Lavoisier, Tec et Doc, Paris, 1993.

[12] Wen C.Y., Fan L.T., Models for flow systems and chemical reactors, Marcel Dekker, Inc., New York, USA, 1975.